Stress intensity factors for embedded elliptical cracks in cylindrical and spherical vessels

Paolo Livieri[1], Fausto Segala[2]
[1]Dept of Engineering, University of Ferrara, via Saragat 1, 44122, Ferrara, Italy,
paolo.livieri@unife.it
[2]Dept of Physics, University of Ferrara, via Saragat 1, 44122, Ferrara, Italy,
fausto.segala@unife.it

ABSTRACT

In this paper, we give a very accurate approximation of the stress intensity factors of embedded elliptical cracks in cylindrical and spherical vessels. We evaluate the stress intensity factor along the whole crack border; we do so using a polynomial weight function based on a second order approximation of the Oore-Burns integral in terms of the deviation of the contour from a disk. The stress intensity factor is given for uniform internal pressure and is related to the hoop stress. Finally, a comparison with FE stress intensity factor is given.

KEYWORDS

three-dimensional cracks, weight function, stress intensity factor, analytic solution

NOMENCLATURE

δ	size of mesh over crack
Ω	crack shape
$\partial\Omega$	crack border
Q	point of Ω
Q'	point of crack border where evaluate the stress intensity factor
P	point of crack border
Δ	distance between Q and $\partial\Omega$
K_I	mode I stress intensity factor
$K_{m\,n}$	dimensionless stress intensity factor
$\bar{x}, \bar{y}$	actual Cartesian coordinate system
x, y	dimensionless Cartesian coordinate system
u, v	auxiliary dimensionless coordinate system
p, p_{mn}	reference constants (pressure)
$\bar{a}, \bar{b}$	actual semi-axis of an elliptical crack
a,b	dimensionless semi-axis of an elliptical crack
e	eccentricity of ellipse $e = \sqrt{1 - \frac{\bar{b}^2}{\bar{a}^2}}$
K(e)	elliptical integral of first kind
E(e)	elliptical integral of second kind
σ_n	nominal tensile stress in $\bar{x}, \bar{y}$ actual Cartesian coordinate system
σ	nominal tensile stress in x, y dimensionless Cartesian coordinate system

1. INTRODUCTION

The assessment of stress intensity factors (SIFs) is a crucial step to calculate the safety of mechanical components. This is one of the three fundamental points of the "fracture mechanics triangle" that considers also loadings and fracture toughness of the material [1].

In mechanical components, many planar flaws are treated, for example lack of fusion in welds, undercuts, sharp groove-like localised corrosion etc. Furthermore, volumetric flaws such as porosity, cavities, solids inclusions should be taken into account as two-dimensional planar flaws so that the fracture mechanics concept can be used to evaluate the safety of components. However, the designer as suggested, for example, by SINTAP/FITNET [1], BS7910 [2] and API 579 [3] can consider a crack shape idealisation and take into account an equivalent crack among a limited number of planar flaws. Usually, the reference cracks have an elliptical shape or are considered as cracks with straight flanks. In the presence of multiple cracks in the same plane close to one another, the iteration effects gives a stress intensity factor larger than the sum of individual cracks; a fictitious re-size of the flow is then necessary. In general, elliptical cracks (embedded cracks or surface cracks) are considered as re-characterisation of actual cracks and increase their theoretical interest in the SIF assessments. This problem is considered by Noguchi et al. [4] in a solid under tension by means of modified force method and by Chai and Zhang [5], who analysed the interactions between surface crack and an embedded elliptical crack in a pressurized cylinder. The analysis was carried out numerically and the results were presented in tabular form to estimate the stress intensity factor. Usually, numerically analysis is taken into account for the assessments of SIF in elliptical cracks in pressure vessels and results are presented in tabular form or by means of new interpolation functions [6-9].

A general weight function for planar flaw in a three-dimensional body is known in the literature as the O-integral, given by Oore and Burns [10]. However, the complexity of the evaluation of the O-integral suggested us to find an approximation in closed analytical form in order to obtain some powerful alternative formulations [11]. Otherwise, a specific numerical procedure it is necessary to obtain accurate results from the O-integral as recently indicate in reference [12]. Anyway, the agreement by numerical procedures and closed expressions, developed by the authors, was always excellent.

In general, the weight function proposed in literature, is obtained from FE results of elliptic or semi-elliptic defects [13-15].

As underlined by Yagawa et al. [8] it is well known that embedded cracks seem more practical and also more probable than initial cracks. For this reason, a closed form solution for embedded elliptical cracks could be useful for estimate the SIF along the whole crack border.

The aim of our paper is to present a closed-form expression of the SIF for embedded elliptical cracks in cylindrical and spherical pressure vessels with inner pressure. The deviation of an ellipse from the disk is quantitatively described by the parameter $\varepsilon = 1 - \bar{b}/\bar{a}$ where $\bar{a}$ and $\bar{b}$ are the major and minor semi-axis, respectively (and therefore in terms of the eccentricity $e = \sqrt{1 - \bar{b}^2 / \bar{a}^2}$, since $A\varepsilon + B\varepsilon^2 \approx \frac{A}{2}e^2 + \frac{1}{4}\left(\frac{A}{2} + B\right)e^4$ with A and B real numbers). The major axis can be inclined with respect to the radial direction. Furthermore, in order to verified the accuracy of new formulations a comparison with FE results is presented.

2. Theoretical background

The stress intensity factor (SIF) of a two dimensional flaw in a three-dimensional body can be evaluated in many different ways (see for example [16-23]). The weight functions technique, introduced by Bueckner [24] and Rice [25], is a method for evaluate the SIF without taking into account the cracks in the numerical simulations. In particular, for an elliptical cracks of equation $(\bar{x},\bar{y})=(\bar{a}\cdot\cos\alpha\ ,\bar{b}\cdot\sin\alpha)$, the SIF can be evaluated with good accuracy by means of the Oore-Burns integral [10]. In previous papers [21-22], the authors discovered the expression of the first and second order expansion with respect to the deviation from the disk of the O-integral for elliptical cracks. Under uniform tensile stress σ the difference ΔK_I, between the classic Irwin solution and Oore-Burns integral, for an ellipse of semi-axis ($\bar{a}$,$\bar{b}$) is given by:

$$\frac{\Delta K_I}{\sigma\sqrt{\bar{a}}}=\frac{\varepsilon}{10\sqrt{\pi}}\left[\cos 2\alpha+\varepsilon\left(-\frac{1}{48}+\frac{1}{4}\cos 2\alpha+\frac{1}{3}\cos 4\alpha\right)\right] \tag{1}$$

where, $\varepsilon=(1-\frac{\bar{b}}{\bar{a}})$. In the case of $\bar{b}/\bar{a}$ =0.7 the gap is less then 2 %.

Let Ω be an open bounded simply connected subset of the plane as in Figure 1 that represents a plane embedded defect. If $Q'=Q'(x,y)\in\partial\Omega$, the SIF at the point Q' is given by [10, 26, 27]:

$$K_I(Q')=\frac{\sqrt{2}}{\pi}\int_\Omega\frac{\sigma_n(Q)}{\sqrt{f(Q)}\ |Q-Q'|^2}d\Omega\ ,\qquad Q'\in\partial\Omega \tag{2}$$

where

$$f(Q)=\int_{\partial\Omega}\frac{ds}{|Q-P(s)|^{2}} \tag{3}$$

In Eq. (2) $Q=Q(x,y)\in\Omega$, s is the arch-length parameter, the point P(s) runs over the boundary $\partial\Omega$ and σ_n(Q) is the nominal tensile loading evaluated without the presence of the crack. A standard calculation shows that $f(Q)\approx\frac{\pi}{\Delta}$ where Δ is the distance between Q and $\partial\Omega$ [27].

In a recent paper, the authors proposed a second order approximation of integral (2) in order to avoid the numerical integration without loss of accuracy.. We recall that near $\partial\Omega$ (see [11] for details) by operating a rigid motion, we may assume Q'=0 and $\partial\Omega$ approximated by the parabola $y=kx^2$ in a small neighbourhood of Q. Now, if we consider an ellipse of semi axis $(\bar{a},\bar{b})$ by means of the linear transformation:

$$\begin{cases} x=\dfrac{\bar{x}}{\bar{a}} \\ y=\dfrac{\bar{y}}{\bar{a}} \end{cases} \tag{4}$$

We may work on dimensionless coordinates (see Fig. 2).

Then, a change of variables of the dimensionless coordinates (x, y) was performed:

$$\begin{cases} x=(1-r\sin\vartheta)\cos\alpha-r\cos\vartheta\sin\alpha \\ y=r\cos\vartheta\cos\alpha+(1-r\sin\vartheta)\sin\alpha \end{cases} \tag{5}$$

where

$$r = 2\sin\vartheta \sin^2\varphi \tag{6}$$

and α is the coordinate of Q' on $\partial\Omega$. In the dimensionless (x,y) coordinate system the nominal stress becomes: $\sigma(x, y) = \sigma_n(x\,a, y\,a)$.

The second order approximation $K_{I,2}$ of integral (2) is given by:

$$K_{I,2} = \frac{4\sqrt{a}}{\pi\sqrt{\pi}} \int \sin\vartheta \cos^2\varphi \left[\sigma - \varepsilon\left(\frac{\partial\sigma}{\partial y} + \sigma Q \right) + \frac{\varepsilon^2}{2}\left(y^2 \frac{\partial^2\sigma}{\partial y^2} + 2y\frac{\partial\sigma}{\partial y} Q + \sigma R \right)\right] d\vartheta d\varphi \tag{7}$$

where the integral is computed on the "longitude" $\vartheta \in [0, \pi]$ and the "latitude" $\varphi \in [0, \pi/2]$. Q and R are functions of $(\alpha, \vartheta, \varphi)$ whose the analytical expression is shown in the appendix. Eqs. (7) can analytically solved or numerically evaluated without particular problems (see ref. [11])

In the case of a circle (ε=0), therefore Eq. (7) reduces to:

$$K_I = \frac{4\sqrt{a}}{\pi\sqrt{\pi}} \int \sin\vartheta \cos^2\varphi \, \sigma \, d\vartheta d\varphi \tag{8}$$

Eq. (8) is the exact weight function of a disk but the singularity disappears tanks to the change of variable (5). This is a strong advantage because in order to overcome the problem of the ingularity we do not need any specific procedure for weight function integration. Note that for a disk, the exact mode I weight function is known and exactly agrees with that proposed by Galin (see Tada et al. [13] and Livieri and Segala [11]). Furthermore, Eq. (8) can be very useful to obtain closed form solutions for the disk [11].

If the nominal stress σ over the crack is a polynomial in (x,y), that is a finite sum of terms of the type $x^m\, y^n$, it is very opportune to explicit Eq. (7). In the special case when $\sigma(x, y) = \sum p_{mn}\, x^m\, y^n$, p_{mn} being a pressure that takes into account the physical dimension of σ and the integral in the r.h.s. of (7) can be easily expressed. We obtain:

$$K_{I,2} = \frac{\sqrt{a}}{\sqrt{\pi}} \sum_{m+n\le 2} p_{mn}\, K_{mn} \tag{9}$$

where

$$K_{00}(\alpha) = 2 - \varepsilon\left(\frac{1}{2}+\frac{2}{5}\cos 2\alpha\right) - \frac{\varepsilon^2}{10}\left(\frac{49}{12}+\cos 2\alpha+\frac{38}{63}\cos 4\alpha\right) \tag{10 a}$$

$$K_{10}(\alpha) = \frac{4}{3}\cos\alpha - \frac{\varepsilon}{5}\left(\cos\alpha+\frac{16}{21}\cos 3\alpha\right) - \frac{29}{35}\varepsilon^2\left(\frac{1}{4}\cos\alpha+\frac{1}{9}\cos 3\alpha+\frac{1}{33}\cos 5\alpha\right) \tag{10 b}$$

$$K_{01}(\alpha) = \frac{4}{3}\sin\alpha - \frac{\varepsilon}{5}\left(9\sin\alpha+\frac{16}{21}\sin 3\alpha\right) + \frac{\varepsilon^2}{35}\left(\frac{27}{4}\sin\alpha+\frac{53}{9}\sin 3\alpha-\frac{29}{33}\sin 5\alpha\right) \tag{10 c}$$

$$\begin{aligned} K_{20}(\alpha) = {} & \frac{2}{3}+\frac{8}{15}\cos 2\alpha - \varepsilon\left(\frac{1}{10}+\frac{16}{105}\cos 2\alpha+\frac{4}{63}\cos 4\alpha\right)+ \\ & -\frac{\varepsilon^2}{5}\left(\frac{29}{56}+\frac{4}{9}\cos 2\alpha+\frac{62}{231}\cos 4\alpha+\frac{164}{3003}\cos 6\alpha\right) \end{aligned} \tag{10 d}$$

$$K_{11}(\alpha) = \frac{8}{15}\sin 2\alpha - \frac{2}{3}\varepsilon\left(\sin 2\alpha+\frac{2}{21}\sin 4\alpha\right) + \frac{\varepsilon^2}{21}\left(\frac{17}{30}\sin 2\alpha+\sin 4\alpha-\frac{164}{715}\sin 6\alpha\right) \tag{10 e}$$

$$\begin{aligned} K_{02}(\alpha) = {} & \frac{2}{3}+\frac{8}{15}\cos 2\alpha + \frac{\varepsilon}{3}\left(\frac{-47}{10}+\frac{124}{35}\cos 2\alpha+\frac{4}{21}\cos 4\alpha\right)+ \\ & +\frac{\varepsilon^2}{21}\left(\frac{837}{40}-\frac{43}{3}\cos 2\alpha-\frac{172}{55}\cos 4\alpha+\frac{164}{715}\cos 6\alpha\right) \end{aligned} \tag{10 f}$$

Therefore, in the Eq. (9) the SIF is analytically computed in terms of the knowledge of coefficients p_{mn}. These parameters should be calculated from FE analysis or from analytical expansion of the stresses such as the case of pressure vessels.

3. Stress intensity for elliptical crack in cylindrical and spherical vessels

The linear elastic solution for stresses in cylindrical or spherical vessels under inner pressure is well known and reported in many textbook (see for example ref. [28]). In this paper formulae for pressure vessels made of linear elastic material will be reported. However, the method can be used also in presence of residual stresses provided that the faces of the crack are opened. For non-linear behaviour of materials, the stress distribution is more complex and requires to take into account the dimension of the plastic zone. For example, after an autofrettage procedure, both loading and unloading phases have been analysed as well as the influence of Bauschinger effect on residual stresses [29-33].

For linear elastic material, the hoop stress σ_θ related to an uniform inner pressure, at distance *r,* is given by:

$$\sigma_\vartheta = \frac{p\,r_i^2}{r_e^2 - r_i^2}\left(1 + \frac{r_e^2}{r^2}\right) \tag{11}$$

for cylindrical vessels, and

$$\sigma_{\vartheta} = \frac{p\, r_i^3}{2\left(r_e^3 - r_i^3\right)}\left(2 + \frac{r_e^3}{r^3}\right) \qquad (12)$$

for spherical vessels.

The reference geometries considered in this paper are shown in Figs. 3 and 4. For a nominal hoop stress σ_θ acting over an elliptical crack of semi-axis $\left(\bar{a}, \bar{b}\right)$, by taking into account the opening mode due to σ_θ stress, we can evaluate the SIF by expanding Eq. (9) up to the second order. The crack considered in the analysis acts in a longitudinal plane *l-r* and with its major-axes rotated of an angle ψ respect to the radial direction *r* (*l* is the longitudinal direction). From Eq. (11), after some calculations, the pressure p_{mn} for cylindrical vessels take the form

$$p_{00} = \frac{p\, r_i^2}{r_e^2 - r_i^2}\left(1 + \frac{r_e^2}{r^2}\right) \qquad (13a)$$

$$p_{10} = \frac{2\, p\; r_i^2\, r_e^2\, \bar{a}\cos\psi}{\left(r_i^2 - r_e^2\right) r^3} \qquad (13b)$$

$$p_{01} = \frac{2\, p\; r_i^2\, r_e^2\, \bar{a}\sin\psi}{\left(r_i^2 - r_e^2\right) r^3} \qquad (13c)$$

$$p_{11} = \frac{6\, p\; r_i^2\, r_e^2\, \bar{a}^2\cos\psi\sin\psi}{\left(r_i^2 - r_e^2\right) r^4} \qquad (13d)$$

$$p_{20} = \frac{3\, p\; r_i^2\, r_e^2\, \bar{a}^2\cos^2\psi}{\left(r_i^2 - r_e^2\right) r^4} \qquad (13e)$$

$$p_{02} = \frac{3\,p\; r_i^2\, r_e^2\, \overline{a}^2 \sin^2\psi}{\left(r_i^2 - r_e^2\right) r^4} \tag{13f}$$

For spherical vessels, from Eqs. (12), by means of a similar procedure, the pressures p_{mn} for spherical vessels subjected to inner pressure take the form

$$p_{00s} = \frac{p\, r_i^3}{2\left(r_e^3 - r_i^3\right)}\left(2 + \frac{r_e^3}{r^3}\right) \tag{14a}$$

$$p_{10s} = \frac{3\,p\, r_i^3 r_e^3 \overline{a}\; p \cos\psi}{2\left(r_i^3 - r_e^3\right) r^4} \tag{14b}$$

$$p_{01s} = \frac{3\,p\, r_i^3 r_e^3 \overline{a}\; p \sin\psi}{2\left(r_i^3 - r_e^3\right) r^4} \tag{14c}$$

$$p_{11s} = \frac{6\,p\, r_i^3 r_e^3 \overline{a}^2\; p \cos\psi \sin\psi}{\left(r_i^3 - r_e^3\right) r^5} \tag{14d}$$

$$p_{20} = \frac{3\,p\; r_i^2\, r_e^2\, \overline{a}^2 \cos^2\psi}{\left(r_i^2 - r_e^2\right) r^4} \tag{14e}$$

$$p_{02} = \frac{3\,p\; r_i^2\, r_e^2\, \overline{a}^2 \sin^2\psi}{\left(r_i^2 - r_e^2\right) r^4} \tag{14f}$$

Figs 5a-c reports the trend of SIF in cylindrical and spherical pressure vessels along the whole crack front for different value of ψ angle. If the SIF is reported in dimensionless form by dividing the SIF by the reference value of K_I at α=0, the SIF of cracks in cylindrical or spherical vessels are very similar despite the different trend of inner pressure with the radius *r* and a great gap in terms of absolute values of SIF.

4. Numerical verifications

In order to carefully evaluate the SIF values predicted by means of Eqs. 9, 10, 13 and 14, an accurate FE analysis has been evaluated. Small size elements were located in the proximity of the crack border. Let us consider two reference cases: a cylinder and a sphere under inner pressure as reported in figures 3 and 4 (the characteristic dimensions r_i and r_e of the two vessels are the same). The considered cracks have circular and elliptical shape and are located exactly in the middle of the wall of thickeness *t*. For circular case $\overline{a}/t$ is equal to 0.05 while for elliptical crack $\overline{b}/\overline{a} = 0.5$ and $\overline{a}/t$ = 0.1. In both cases the crack can be considered with good accuracy as an embedded crack in a infinite body. The stress, near the crack border, tends toward infinit with a power low of the type: $r^{0.5}$, where *r* is the distance from the notch tip [34]. Fortunately, these highly stresses zones are usually very small in comparison to the remaining part of the structure. Figure 6 shows a typical mesh used to evaluate the SIF. The three-dimensional analysis was carried out by using the smallest element about 10^{-6} -10^{-5} times the thickness of the vessel. The stress intensity factors was evaluated on the basis of asymptotic proprieties of the stress field near the notch raiser. This way forces the use of very fine mesh in the neighbourhood of the interest point but with the advantage to obtain very accurate results [35]. Figure 7 shows the trend of the hoop stress σ_θ along the radial directions. The slope is very close to the theoretical value of 0.5. On the basis of SIF definition we can obtain K_I by the following simple equation:

$$K_I = \sqrt{2\pi} \lim_{d \to 0^+} d^{0.5} \sigma_\theta \qquad (15)$$

where σ_θ is the hoop stress evaluated in direction *d* perpendicular to the elliptical border.

Tables 1 and 2 repots a comparison among the proposed equations and FE analysis in three characteristic points. The agreement is satisfactory for the use in engineering field. The difference between FE results and analytical ones for circular cracks is around 2%, whereas for $\bar{b}/\bar{a} = 0.5$ the gap increasing up to the 5 % with respect to the maximum value of K_I.

5. CONCLUSIONS

The main conclusions obtained in this paper for embedded elliptical cracks in cylindrical and spherical vessels are the following:

- The proposed equations are very suitable for the assessments of stress intensity factors of embedded elliptical cracks in pressure vessels along the whole crack border. The crack lies in the longitudinal plane with its major axis inclined with respect to the radial direction.
- For circular cracks the proposed solution is exact. Thanks to a change of variable coordinates the singularity of the weight functions was removed. So that, the integration requires only a standard software without the use of any particular algorithms.
- The shape of the SIF along the crack border is virtually the same for embedded cracks in cylindrical or spherical vessels.

6. APPENDIX

The explicit values of Q and R from reference [11] results:

$$Q(\alpha,\vartheta,\varphi)=\frac{1}{4}-\left(\frac{1}{4}+\cos 2\vartheta-\frac{r}{2}\sin\vartheta-\frac{r^2}{4}\cos 2\vartheta\right)\cos 2\alpha+\left(\sin 2\vartheta+\frac{r}{2}\cos\vartheta-\frac{r^2}{4}\sin 2\vartheta\right)\sin 2\alpha \tag{A1}$$

$$R=\begin{Bmatrix} -\frac{5}{8}+\frac{\rho^2}{4}-\frac{\rho^4}{16}+\frac{5}{32}(A^2+B^2)+\frac{AM+BN}{4}+\left(\frac{A}{8}+\frac{M}{2}\right)\cos 2\alpha-\left(\frac{B}{8}+\frac{N}{2}\right)\sin 2\alpha+ \\ \left[\frac{5}{32}(A^2-B^2)+\frac{AM-BN}{4}+M^2-N^2\right]\cos 4\alpha-\left[\frac{5}{16}AB+\frac{AN+BM}{4}+2MN\right]\sin 4\alpha \end{Bmatrix} \tag{A2}$$

By the definitions of A, B, M and N we are able to express all the coefficients in (A1 and A2) in terms of (r,θ).

$$A=1-2r\sin\vartheta-r^2\cos 2\vartheta \tag{A3}$$

$$B=2r\cos\vartheta-r^2\sin 2\vartheta \tag{A4}$$

$$M=\cos 2\vartheta \tag{A5}$$

$$N=\sin 2\vartheta \tag{A6}$$

$$\sqrt{1-\rho^2}=\sqrt{r}\,\sqrt{2\sin\vartheta-r} \tag{A7}$$

Table 1 Comparison between Oore-Burns' integral and FE result (mesh for Riemann' sum with incremental angle $\delta=\pi/1600$; p is the reference pressure, cylinder: r_i=80 mm, r_e=120 mm)

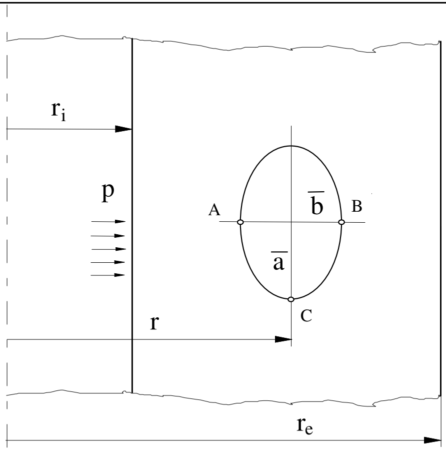

		point	$\frac{K_I}{p\sqrt{\bar{a}}}$ Riemann' sum of Eq. (2) with numerical procedure [12]	FE analysis	$\frac{K_{I,2}}{p\sqrt{\bar{a}}}$ Eqs. (9, 10 and 13) Second order approximation	$\frac{K_{I,2}}{p\sqrt{\bar{a}}}$ Eqs. (8 and 11) Exact solution (only for circle)
$\bar{b}/\bar{a}$	$\bar{a}$ [mm]					
0.5	4	C	1.50	1.40	1.55	-
0.5	4	B	1.94	1.98	2.02	-
0.5	4	A	2.00	2.03	2.07	-
1	2	C	2.20	-	2.20	2.20
1	2	B	2.17	-	2.17	2.17
1	2	A	2.24	2.19	2.24	2.24

Table 2 Comparison between Oore-Burns' integral and FE result (mesh for Riemann' sum with incremental angle $\delta=\pi/1600$; p is the reference pressure, sphere: r_i=80 mm, r_e=120 mm)

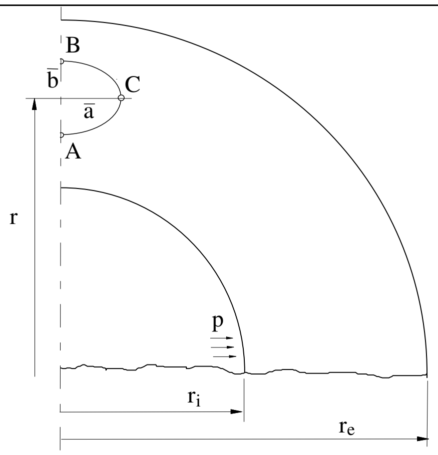

		point	$\frac{K_I}{p\sqrt{\bar{a}}}$ Riemann' sum of Eq. (2) with numerical procedure [12]	FE analysis	$\frac{K_{I,2}}{p\sqrt{\bar{a}}}$ Eqs. (9, 10 and 14) Second order approximation	$\frac{K_{I,2}}{p\sqrt{\bar{a}}}$ Eqs. (8 and 12) Exact solution (only for circle)
$\bar{b}/\bar{a}$	$\bar{a}$ [mm]					
0.5	4	C	0.604	0.561	0.628	-
0.5	4	B	0.780	0.795	0.807	-
0.5	4	A	0.806	0.813	0.832	-
1	2	C	0.886	-	0.887	0.886
1	2	B	0.870	-	0.869	0.870
1	2	A	0.903	0.883	0.902	0.903

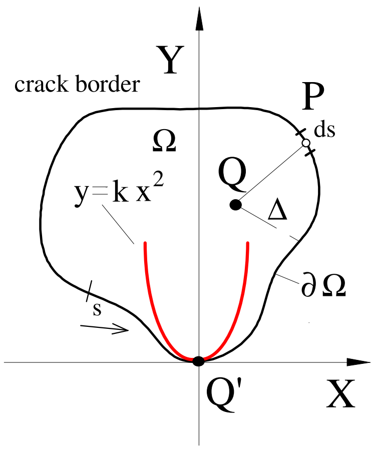

Figure 1. Crack shape Ω and local approximation

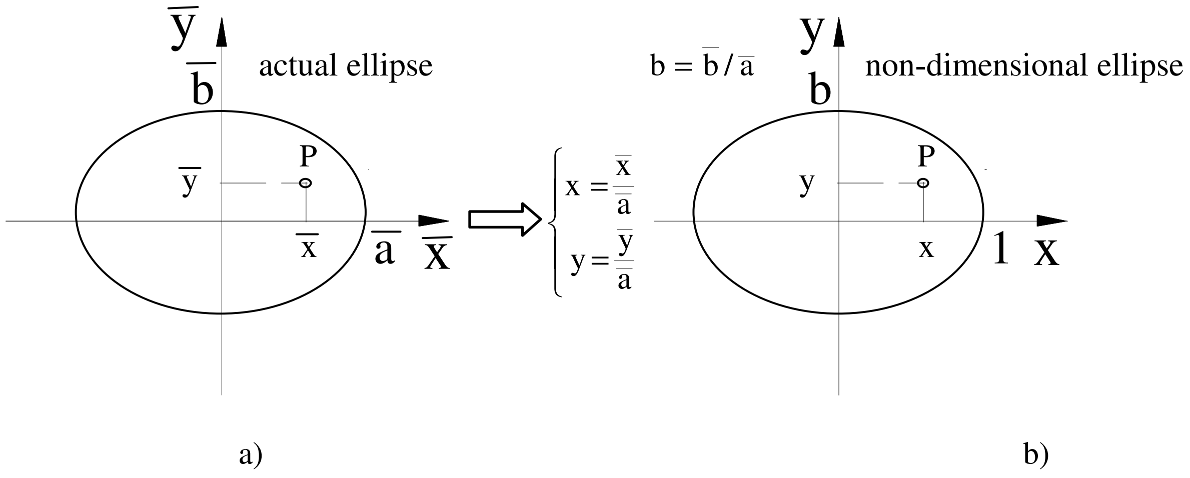

Figure 2. a) Actual elliptical crack; b) dimensionless elliptical crack

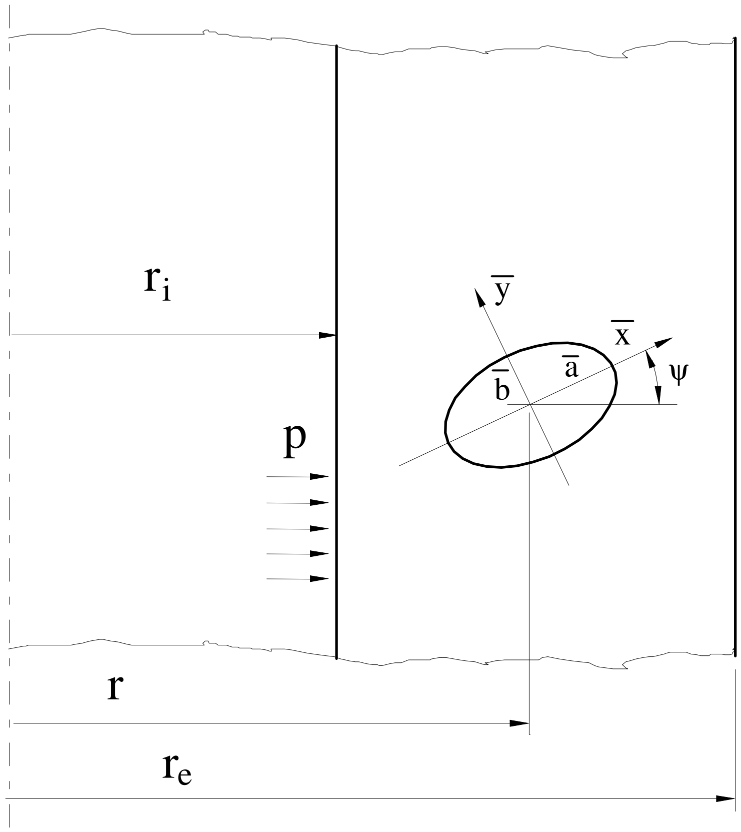

Figure 3. Reference cylindrical pressure vessel

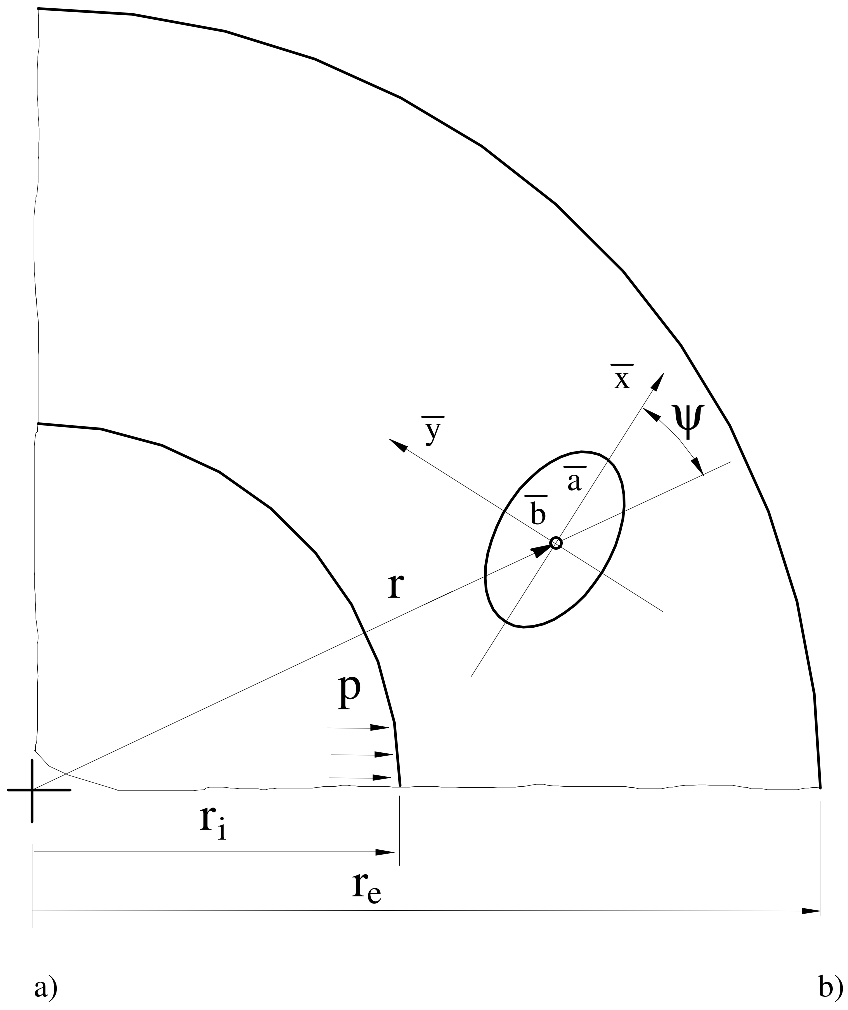

Figure 4. Reference spherical pressure vessel

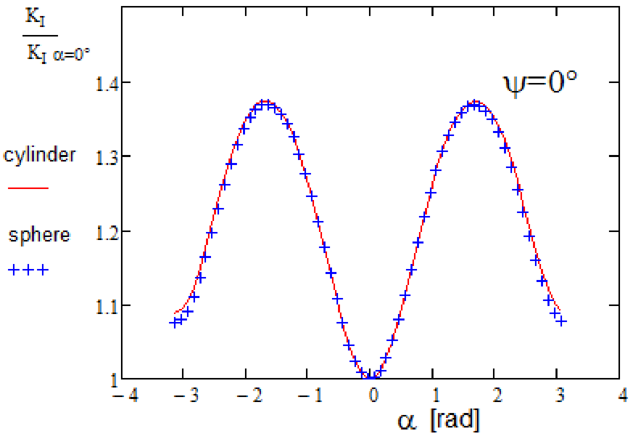

a

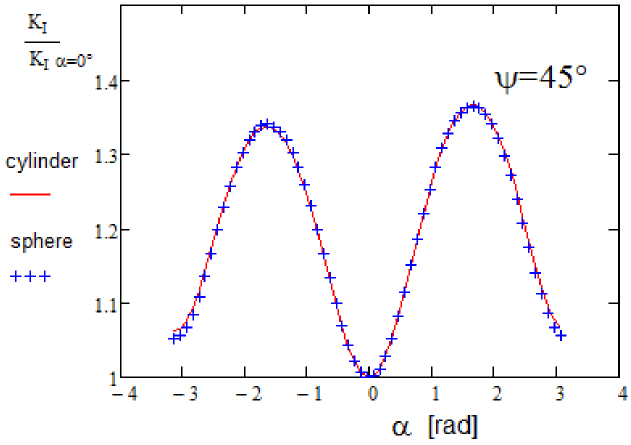

b

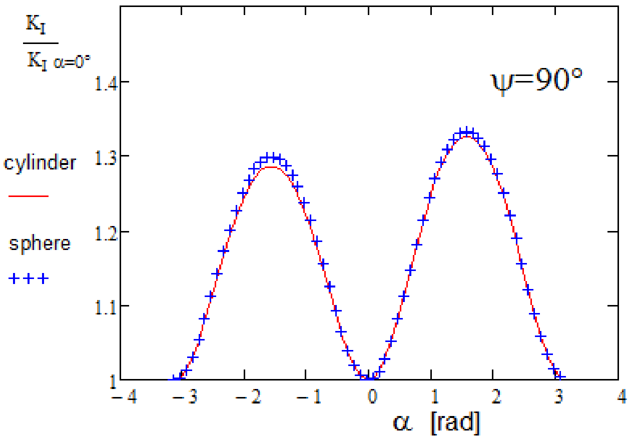

c

Figure 5. Stress intensity factors for cylindrical and spherical vessels subjected to inner pressure for different angle ψ ($\overline{a}$ = 4 mm, $\overline{b}$ = 2 mm; r_i=80 mm , r_e=120 mm)

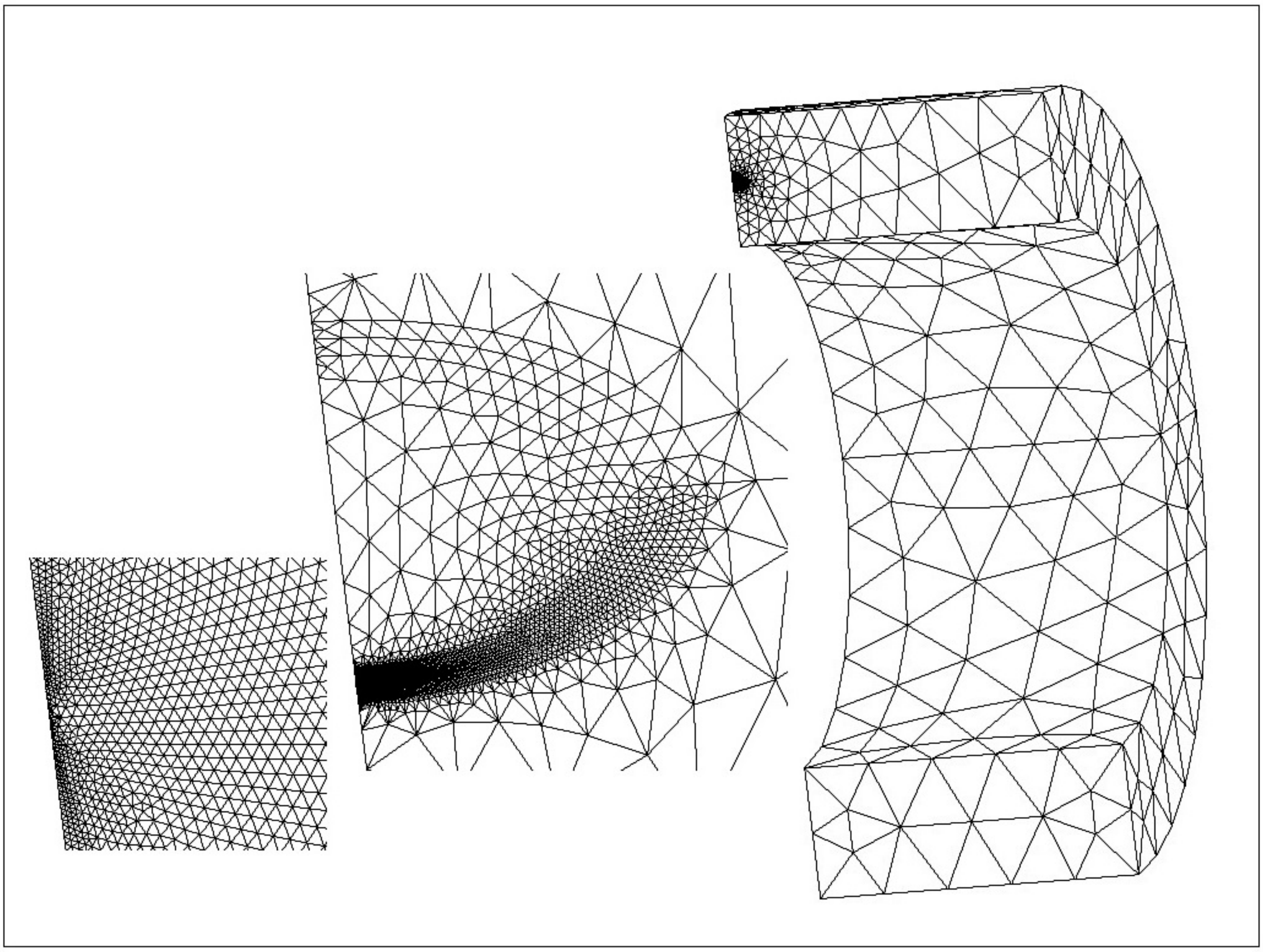

Figure 6. Typical mesh used in the FE analysis

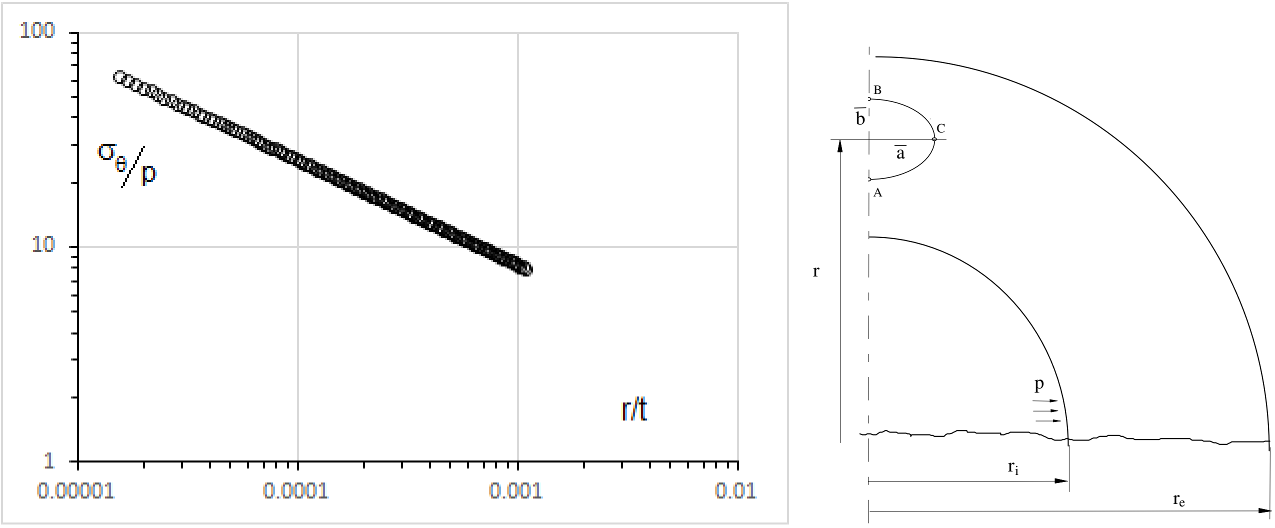

Figure 7. Hoop stress along radial direction point A (r_i=40 mm, r_e=120 mm, $\bar{a}$ = 4 mm, $\bar{b}$ = 2 mm)

REFERENCES

1 U. Zerbst, M. Schödel, S. Webster, R. Ainsworth, Fitness-for-Service Fracture Assessment of Structures Containing Cracks: A Workbook based on the European SINTAP/FITNET procedure, Elsevier, 1st ed. Oxford, Amsterdam, the Netherlands 2007.

2 BS 7910, Guide on Methods for Assessing the Acceptability of Flaws in Metallic Structures, British Standard Institution, London, 2005.

3 API 579, Recommended Practice for Fitness for Service, American Petroleum Institute (API), Washington, 2000.

4 H. Noguchi, R.A. Smith, J.J. Carruthers, M.D. Gilchrist, Stress intensity factors of embedded elliptical cracks and an assessment of the ASME XI defect recharacterisation criteria. International Journal of Pressure Vessels and Piping, 70(1), 69-76, 1997.

5 G. Chai, K. Zhang, Stress intensity factors for interaction of surface crack and embedded crack in a cylindrical pressure vessel, International Journal of Pressure Vessels and Piping, Volume 77, 9(1), 539-548, 2000.

6 Xudong Qian, K_I–T estimations for embedded flaws in pipes – Part I: Axially oriented cracks. International Journal of Pressure Vessels and Piping, 87(4), 134-149, 2010.

7 Xudong Qian, K_I–T estimation for embedded flaws in pipes – Part II: Circumferentially oriented cracks, International Journal of Pressure Vessels and Piping, 87(4), 150-164, 2010.

8 G. Yagawa, Y. Kanto, S. Yoshimura Probabilistic fracture mechanisc of nuclear structural components: consideration of transition from embedded crack to surface crack. Nuclear Engineering and Design, 191, 263-273, 1999.

9 G. Chai, K. Zhang, D. Wu, Analyses on interactions of two identical semi-elliptical surface cracks in the internal surface of a cylindrical pressure vessel. International Journal of Pressure Vessels and Piping, 67(2), 203-210, 1996.

10 M. Oore, D.J. Burns. Estimation of stress intensity factors for embedded irregular cracks subjected to arbitrary normal stress fields. Journal of Pressure Vessel Technology ASME 102, 202–211, 1980.

11 P. Livieri, F. Segala, New weight functions and second order approximation of the Oore-Burns integral for elliptical cracks subject to arbitrary normal stress field. Engineering Fracture Mechanics, 138, 100-117, 2015.

12 P. Livieri, F. Segala. Sharp evaluation of the Oore-Burns integral for cracks subjected to arbitrary normal stress field, Fatigue & Fracture of Engineering Materials & Structures, 2014, 37, pp 95–106.

13 H. Tada, C.P. Paris, G.R. Irwin. The stress analysis of cracks handbook. Third edition, ASME press, 2000.

14 X.J. Zheng, G. Glinka, R.N. Dubey. Calculation of stress intensity factors for semielliptical cracks in a thick-wall cylinder, International Journal of Pressure Vessels and Piping, 62(3), 249–258, 1995.

15 M. Beghini, L. Bertini, A. Gentili. An explicit weight function for semi-elliptical surface cracks. ASME, Journal of Pressure Vessel Technology, 119, 216–223, 1997.

16 P. H. Wen, M. H. Aliabadi, D P. Rooke. Mixed-mode weight functions in three-dimensional fracture mechanics: static, Engineering Fracture Mechanics, 59(5), 563–575, 1998.

17 J.L. Desjardins, D.J. Burns, J.C. Thompson. A weight function technique for estimating stress intensity factors for cracks in high pressure, Journal of pressure Vessel Technology, ASME, 113, 10–21, 1991.

18 A.A. Al-Falou, R.C. Ball. The 3-D weight functions for a quasi-static planar crack, International Journal of Solids and Structures, 37(37), 5079–5096, 2000.

19 Y. Murakami, M. Endo. Quantitative evaluation of fatigue strength of metals containing various small defects or cracks. Engineering Fracture Mechanics, 17 (1), 1–15, 1993.

20 J.R. Rice. Weight function theory for three-dimensional elastic crack analysis. ASTM STP1020, R.P. Wei and R.P. Gangloff. Eds. Philadelphia, American Society for Testing and Materials, 29–57, 1989.

21 P. Livieri, F. Segala. First order Oore–Burns integral for nearly circular cracks under uniform tensile loading, International Journal of Solids and Structures, 47 (9), 1167–1176, 2010.

22 P. Livieri, F. Segala, Evaluation of Stress Intensity Factors from elliptical notches under mixed mode loadings. Engineering Fracture Mechanics, 81, 110-119, 2012.

23 A. Salvadori, F. Fantoni. Weight function theory and variational formulations for three-dimensional plane elastic cracks advancing, International Journal of Solids and Structures, 51(1) 1030–1045, 2014.

24 H.F. Bueckner. A novel principle for the computation of stress intensity factors, ZAMM 50, 529–546, 1970.

25 J.R. Rice. Some remarks on elastic crack-tip stress field. International Journal of Solids and structures, 8(6), 751–758, 1972.

26 P. Livieri, F. Segala, O. Ascenzi. Analytic evaluation of the difference between Oore-Burns and Irwin stress intensity factor for elliptical cracks, Acta Mechanica, 176 (1-2), 95–105, 2005.

27 O. Ascenzi, L. Pareschi, F. Segala. A precise computation of stress intensity factor on the front of a convex planar crack. International Journal for numerical methods in Engineering, 2002, 54, 241–261, 2002.

28 W. C. Young, R. G. Budynas, Roark's Formulas for Stress and Strain, Seventh Edition, McGraw-Hill, 2002.

29 P. Lazzarin, P. Livieri: "Different Solution for Stress and Strain Fields in Autofrettaged Thick-Walled Cylinders", International Journal of Pressure Vessels and Piping, 71 (3), 231-238, 1997.

30 P. Livieri, P. Lazzarin: "Autofrettaged cylindrical vessels and Bauschinger effect: an analytical frame for evaluating residual stress distributions", ASME- Journal of Pressure Vessel Technology, 124, 38-46, 2002.

31 R. Adibi-Asl, P. Livieri, Analytical Approach in Autofrettaged Spherical Pressure Vessels Considering the Bauschinger Effect, ASME- Journal of Pressure Vessel Technology, 129, 411-419, 2007.

32 DWA. Rees. A theory of autofrettage with applications to creep and fatigue. International Journal of Pressure Vessels and Piping, 30, 57-76, 1987.

33 A. Stacey, GA. Webster, Determination of residual stress distributions in autofrettaged tubing. International Journal of Pressure Vessels and Piping 31, 205-220, 1988.

34 G.R. Irwin. Crack-extension force for a part-through crack in a plate. ASME, Journal of Applied Mechanics, 29(4), 651–654, 1962.

35 P. Livieri; F. Berto, P. Lazzarin. Local strain energy approach applied to fatigue analysis of welded rectangular hollow section joints. International Journal of Materials & Product Technology, 30(1/2/3), 124 – 140, 2007.